***In this study, an investigation into the impact of heat transmission in the welded junction of SUS304 pipe has been carried out with the use of a numerical method. An investigation was carried out by employing ANSYS's static structural tools in conjunction with the software package's thermal transient analysis. Based on the heat flow on the welding point, where the temperature reaches 507 °C within 200 mm of the end of the welded pipe, an examination into the efficiency of heat transfer has been carried out. This analysis was based on the heat flow on the welding point. As the total heat flux approaches 7.02e6 W·m$^{-2}$, studies have been conducted on the topic. There have been three types of directional heat flux measurements made (X, Y, and Z), with the numerical findings indicating that the X direction produces the most variable heat flow readings. These checks were performed in a variety of settings. These were chosen as the correct paths to go since they led directly to the source of the warmth. whereas the Z-axis permits the minimum amount of heat flow throughout the board. The damaged area identified on the trees that were still standing was factored into the calculation. To calculate the amount of residual stress, the Von Mises stress was applied repeatedly during the whole procedure. This tactic ended up being employed. Due to the tension caused by the pipe's increased bending radius, the piece of pipe located 200 mm from the pipe's distal end is the most vulnerable. The value was calculated to be 2.49e6 Pa when the temperature was increased to 500 °C***

***Keywords: heat transfer, SUS304, heat flux: welded joint, friction stir welding***

UDC 620
DOI: 10.15587/1729-4061.2023.290124

# IDENTIFYING SOME REGULARITIES OF THE HEAT TRANSFER IN THE WELDED JOINT OF SUS304 PIPE USING A NUMERICAL APPROACH

**Abbas Naseer Hasein**
Lecturer*
**Ashham Mohammed Aned**
*Corresponding author*
Lecturer*
E-mail: ashham.m@mtu.edu.iq
**Mortadha Kareem A. Razzaq**
Lecturer*
*Department of Mechanical Technical/Production
Al-Kut Technical Institute
Middle Technical University
Al-Za'franiya, Baghdad, Iraq, 10074

*Received date 10.08.2023*
*Accepted date 13.10.2023*
*Published date 30.10.2023*

***How to Cite:*** *Hasein, A. N., Aned, A. M., Razzaq, M. K. A. (2023). Identifying some regularities of the heat transfer in the welded joint of SUS304 pipe using a numerical approach. Eastern-European Journal of Enterprise Technologies, 5 (1 (125)), 104–113. doi: https://doi.org/10.15587/1729-4061.2023.290124*

## 1. Introduction

Pipe lining is a difficult task that requires a two-stage welding procedure. With a weld overlay, the repaired section of liner may be permanently sealed off and made to sit flat with the pipe's outside. As a result, the liner is securely fastened to the steel skeleton [1]. The two lined pipes are then joined with a girth weld. The heat fields and residual strains created by such welded connections must be taken into consideration when calculating the structural integrity and expected lifetime of the lined pipe. Physical testing can be replaced by computer approaches based on the Finite Element Method (FEM) [2]. The multiple hurdles make it impractical, time-consuming, and expensive to do experimental research on welding covered pipes [3].

More than twenty-five years ago, [4] proposed analyzing the thermomechanical effects of circumferential butt-welding in three dimensions. C-Mn single-pass model testing verified a similar FEM-based model developed in an earlier set of studies [5, 6]. The nonlinear analysis finite element algorithm ABAQUS was created by numerical modeling of several multi-pass girth-butt-welded stainless steel joints [7]. Accurate prediction of butt-welded steel pipes' thermal history and residual stresses has been made possible by advancements in three-dimensional finite element (FE) modeling during the past decade. In [8], the temperature history and residual stresses in multi-pass girth welds of SUS304 stainless steel pipe sections were investigated using a mixture of 3-D and 2-D FE models. It is possible to get findings that agree well with experimental data because to ABAQUS's three-dimensional simulation capabilities. Using ANSYS, the team at [9] simulated a sphere made of A240-TP304 stainless steel and A106-B carbon steel connected in a variety of ways. Let's investigate how heating a material alters the distribution of residual stress by investigating the role played by thermomechanical behavior. Excellent agreement was found between ANSYS hole-drilling simulations and experimental results. Numerous factors can influence the outcomes of thermal and mechanical assessments [10]. Materials, heat input, welding pool shape, boundaries, and welding order are all variables to consider. In order to ensure that a welding simulation for several materials was accurate, this research utilized both austenitic stainless steel pipe and low alloy steel pipe. The absence of the weld cladding layer underneath the low alloy steel joint may account for discrepancies between the predicted and experimental findings [11].

Therefore, studies on the development of heat transmission in the welded junction of SUS304 pipe are scientific relevance.

## 2. Literature review and problem statement

Their welding technique includes a heating and cooling cycle that directly affects the reliability and durability of the welded component after it is placed into use. The welding

process involves a heating and cooling cycle, therefore this is inevitable. The oil and gas industry, together with thermal power facilities, nuclear power plants, and the pipe networks for boiling water reactors are regular users of circumferential butt welding. The oil and gas pipeline systems are another common user [12].

Research [13] shows that residual strains arise in the area surrounding the weld zone as a result of the thermal cycle, which consists of localized heating and cooling. The potential for a time-dependent failure is amplified when residual stresses are present. According to the information presented, tensile residual stresses can result in stress corrosion cracking and brittle fracture. In addition, the likelihood of a brittle fracture is discussed in reference [14]. Because of the presence of tensile residual stresses inside the material, any fracture, regardless of how little it was to begin with, will get larger as a result of the influence of fatigue loading. The effects of creep and fatigue loading at high temperatures on superalloy materials were studied by researchers from [15]. Microscale cracking may be traced back to the presence of Type-II and Type-III residual stresses, as was theorized by the researchers. Turbine engines, superheater sections, and reheater sections are crucial to the production of electrical power, despite having to function under hazardous conditions. High-performance nickel-based superalloys are ideal for usage in extreme conditions like these. The high temperatures present in industries like nuclear power, thermal power, and aerospace may find nickel-based superalloys to be a suitable alternative [16]. The potential for temperatures of several thousand degrees Fahrenheit is included in this category. Components of a AUSC power plant are fabricated from high-performance materials that are able to tolerate high temperatures without suffering any degradation in their inherent properties. Nickel-based superalloys can withstand temperatures 760 °C greater than steel can (620 °C) [17]. Steel can only withstand temperatures of 620 °C. Because of their high creep strength and resistance to oxidation, Ni-based superalloys like Alloy 617, Alloy 625, and Alloy 263 are favored for use in AUSC power plants. This is demonstrated in [18], which explains why this preference exists. It is essential, however, to keep in mind that the cost of Inconel alloys is higher than that of standard steels containing 9 % Cr. Applications that have a maximum operating temperature of 650 °C commonly make use of ferritic/martensitic grade 12 % Cr steels [19], which are known for their affordability. Modern AUSC power plants frequently employ dissimilar welded connections between 9–12 % Cr steels and Inconel alloys for thick-section components like steam pipes and turbine rotors. Large residual stresses along weldments are caused by differences in the mechanical, chemical, and thermo-physical characteristics of the materials being welded [20]. Residual strains in welds that link together incompatible materials must be carefully managed to guarantee the end product may be utilized safely.

Common applications of HW-TIG, an abbreviation for «hot wire tungsten inert gas welding», include the fabrication of pressure vessels, the construction of ships, and the generation of nuclear power. When compared to traditional TIG welding, HW-TIG may allow for a substantially quicker deposition of weld metal. According to studies published in [21], the microstructure of the Heat-Affected Zone (HAZ) produced by HW-TIG is comparable to that of traditional TIG welding. One possible advantage of HW-TIG welding is that the filler material may be preheated before being added to the weld pool. Relatively low residual stresses are formed close to the weld zone and the HAZ when metal deposition rates are restricted, as described in [22]. This can also result in a decrease in the amount of heat input. There is a possibility of residual tensile stresses developing during either manual TIG welding or HW-TIG welding. If you are aware of the stresses that are formed during the welding process, you may potentially enhance your efficiency and ensure that the welded structure as a whole is adjusted appropriately.

There are a wide variety of non-destructive methods that may be used to determine residual stresses. X-ray diffraction, neutron diffraction, and ultrasonic testing are all examples of such methods. Bragg's rule is used to quantify elastic strains, whereas Hooke's law is used to measure stresses in EBSD and ND. Both of these rules are written by William Bragg. Similar to ND, XRD can assess stress levels down to just 1 mm [23]. Residual tensions one to three millimeters below the surface may be revealed by destructive operations such as Blind Hole Drilling (BHD), Ring Core, Slitting, and Contour Methods. In order to determine residual stress in materials of various thicknesses, the BHD approach has been applied [24]. The application of finite element models to the prediction of weld-induced residual stresses in circumferentially welded butt joints has grown in popularity in recent years. These models have been used for analyzing weld deposits. Some of the writers [25] used computational research with the ABAQUS FE software to validate experimental results on the estimate of residual stresses in ferritic steel welded pipes. The purpose of this study was to double-check the results of the earlier studies. The numerical results they got were quite close to what was seen in the real world. After conducting numerical study with ANSYS FE into the impact of tacking and root gap on the weld-induced residual stress of pipe flange joints, the authors used the BHD approach to validate their findings. [26] Welded pipe joints composed of 2.25Cr-1Mo ferritic steel and SS-316 steel had their surface residual stress distributed using the XRD technique. A106B C-steel and A240-TP304SS steel were used to examine the residual stress in a welded pipe connection [27]. Using an ANSYS FE model that accounted for strain hardening, it was discovered that the peak residual stress of weld metal was much higher than the yield stress of the parent material. For a dissimilar welded connection between P91 and SS304L steel, the authors [28] used the DHD method to examine the residual stress distribution over the weldment thickness. Weld metal has the lowest residual stress level when ranked from highest to lowest [29]. The residual stress values obtained from testing a dissimilar weld composed of P92/SS304L steel/IN625 filler were consistent with those presented in [30]. According to [31], the process of welding results in intricate stress distribution patterns because of the mechanical and thermophysical variations that exist between the base materials. The stress gradients in the fusion zone can become fairly severe when there is a considerable difference in TEC between the two regions. The application of heat treatment has the potential to alleviate some of these strains, but it may not be able to eradicate all of them totally. In this study, let's investigate the influence of post-weld heat treatment (PWHT) on stress relaxation in a P91 welded joint by making use of the parametric ABAQUS FE numerical tool [32]. As a component of the phase-transformation effects, the modeled changes included those that occurred in volume and plasticity during the transition. Through the use of simulation, it is possible to analyze the commencement of

the residual stress as well as its relationship to the material type, preheating, and the number of weld passes. It was discovered that the weld passes had a less influence on the outside wall of the pipe as compared to the inner wall. When the preheating temperatures were elevated from 225 to 325 °C, there was also a decrease in the amount of residual stress that was observed [33].

Therefore, computational methods were utilized in this study in order to explore the impact of heat transfer in the welded connection of SUS304 pipe.

## 3. The aim and objectives of the study

The study aims to identify the heat transfer in the welded joint of SUS304 pipe using a numerical approach.

To achieve this aim, the following objectives are accomplished:

– to investigate the heat transfer efficiency;
– to investigate heat flux due to temperature;
– to calculate residual stresses in the welded spot.

## 4. Research methodology

### 4. 1. Object and hypothesis of the study

The study's object is heat transmission at the welded connection of SUS304 pipes. The goal of the research is to gain an understanding of the temperature distribution and heat flux within the welded joint. The study also investigates the effectiveness of heat transmission in this setting. The effects of heat transfer, directional heat flux measurements, and residual stress on welding SUS304 pipes are analyzed. The final objective is to learn more about the dynamics of heat transfer in such welded joints and the thermal effects that arise from that transfer, and how those dynamics affect the joints' structural integrity and performance.

Measurements of temperature, heat flux, and the orientation of heat flow are hypothesized to have significant effects on the rate of heat transfer within the welded junction of SUS304 pipes. Residual stress in the welded joint is hypothesized to be impacted by temperature and pipe bending radius, and the X-directional heat flow is hypothesized to demonstrate the most significant fluctuation across different measurements. Constant and uniform material characteristics, steady-state circumstances, flawless welds, and isotropic material behavior are among the presumptions made. By assuming two-dimensional heat transport, linear material behavior, and the use of Von Mises stress to describe complicated stress states, the analysis is also made simpler in this work. These presumptions, generalizations, and short cuts set the stage for the research study and analysis.

### 4. 2. Mechanical and thermal properties of SUS304

The material qualities offered are critical for understanding a material's behavior. These properties collectively inform engineering design and analysis, with a Young's Modulus of 210 GPa indicating stiffness. a Poisson's Ratio of 0.27 governing deformation, a density of 7860 kg/m$^3$ defining mass distribution. A specific heat of 444 J/kg K quantifying thermal energy storage, and a thermal conductivity of 50 W/m K dictating heat transfer efficiency as shown in Table 1.

These are critical in forecasting deformation under load, monitoring temperature reactions, and directing material selection for structures and components to achieve optimal performance and dependability under a variety of situations.

Table 1

Mechanical and thermal properties of SUS304

| Young's modulus (GPa) | Passion ratio | Density (kg/m$^3$) | Specific heat (J/kg K) | Conductivity (W/m K) |
|---|---|---|---|---|
| 210 | 0.27 | 7860 | 444 | 50 |

### 4. 3. Primary boundary condition

The welding technique will take place at the location on the pipe that is precisely in the middle of the pipe. It is located a distance of two hundred millimeters (mm) from the terminus of the pipe. A thermal transient was used in conjunction with a static structure in the Ansys software in order to represent the flow of heat as it moved through a system.

### 4. 4. Geometry and mesh

It was able to execute and statistically examine hollow pipe shape with the help of AutoCAD as shown in Fig. 1.

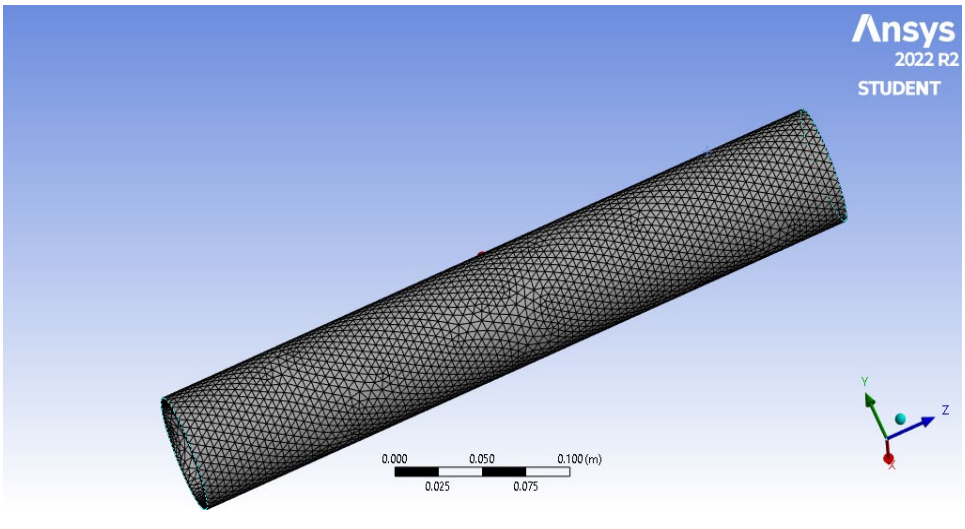


Fig. 1. Meshed model of SUS304

There is a gap in the center, corresponding to the plain portion's beginning and ending. ANSYS, Inc. In order to complete the meshing technique for this particular issue, the creation of mesh was utilized. The particle count of a model is reduced throughout the production of the mesh, going from an unlimited quantity to a range that is easier to work with. To guarantee that the simulations are realistic, a very fine mesh was built by using a rigid grid. As a consequence of this fact, the mesh may be produced. In order to achieve the desired outcome of a fine mesh, careful control of the curvature size by means of a coarse mesh and the element size by means of face meshing was required. Because of this, it was possible to manufacture the needed tiny mesh. The wedge now has a grand total of 553,345 binary nodes across all of its zones. These nodes were produced in the wedge. A sample of this kind of mesh that has been constructed in a two-dimensional context is shown in Fig. 1.

A single side of the model has been built and sculpted so far due to the symmetry that is inherent in the 3D wedge. This conclusion materialized as a happy consequence of a chain of occurrences that uncovered the symmetrical structure of the three-dimensional wedge.

### 4. 5. Grid independent study

Figure *x* depicts the grid-independent research for the process that is currently being simulated. The temperature during the procedure was kept at 500 °C. The von Mises stress is 6e6 Pa, and the total number of components is 23884. The value of the von Mises stress is calculated to be 6.2e6 Pa when the number of components reaches 23973. The shift in the von miss stress does not take place once element 24553 has been reached. As a result, the number of elements that make up the mesh will remain the same, and calculations will be carried out using these particular element counts (24553) as shown in Fig. 2.

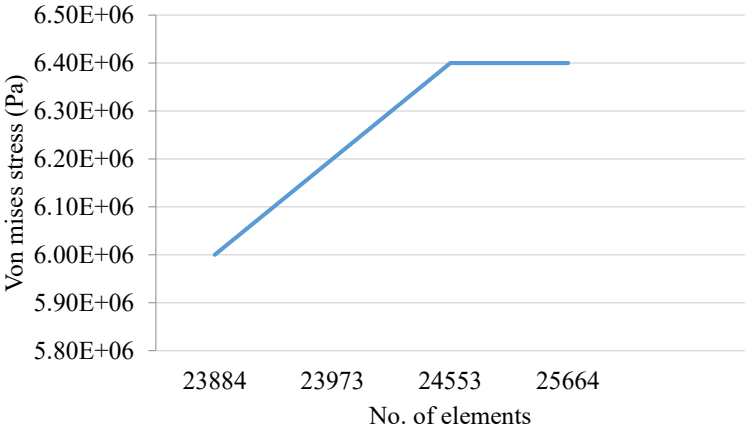


Fig. 2. Grid independent study

Different grid numbers and resolutions are utilized during the testing phase in order to determine how well a numerical or computational model performs and how accurate its results are. In these simulations, the mesh that was utilized to discretize the issue domain has the potential to have a considerable influence on the outcomes. An objective of a test that is not reliant on the grid has been to assess whether or not the answer that is achieved from a simulation continues to be consistent and converges to a trustworthy result no matter how the grid is modified.

## 5. Results of the influence of heat transfer in the welded joint of SUS304 pipe

### 5. 1. Heat transfer efficiency

The thermal behavior of a SUS304 pipe during welding is represented by the Fig. 3, which denotes precise temperature values at various places along the length of the pipe. The length of the pipe measures 400 mm, and the welding process results in a maximum temperature of 507 °C at the welding junction, which is situated 200 mm away from one end of the pipe. As one progresses from the welding point toward the periphery of the pipe, there is a steady reduction in temperature. The temperature at a distance of 195 mm from the welding site is recorded as 500 °C, but at the periphery of the pipe, the temperature is seen to be 20 °C.

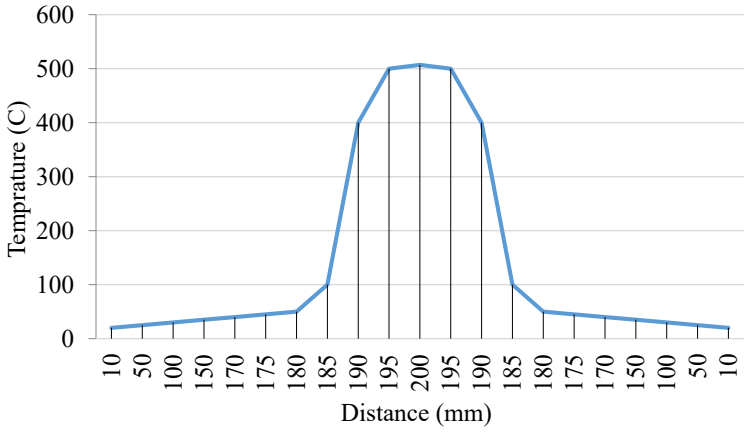


Fig. 3. Heat distribution along the pipe

The observed temperature distribution can be elucidated by the application of heat conduction concepts in material systems. The use of intense heat during the welding process induces a temperature differential throughout the pipe. The observed phenomenon of the temperature decreasing to 500 °C within a distance of 5 mm from the welding spot (specifically at a distance of 195 mm) signifies the fast dissipation of heat. The observed decrease in temperature from 500 °C at a distance of 195 mm to 20 °C at the periphery of the pipe indicates efficient heat dissipation over the whole length of the pipe.

The thermal characteristics of the SUS304 material exert an impact on its behavior under these given conditions. The material's thermal conductivity, which is quite high, facilitates effective heat transfer, resulting in a drop in temperature as heat propagates down the pipe.

Moreover, the thermal capacity of SUS304 significantly influences its ability to absorb energy and its rate of heating or cooling.

The simulated findings generated from ANSYS offer significant insights into the transient thermal dynamics of the pipe throughout and following the welding procedure. The provided information is of utmost importance in evaluating potential structural consequences, such as thermal stress

and expansion effects, that may occur as a result of an uneven distribution of temperature. Additionally, it allows the anticipation of the material's response to high-temperature circumstances, empowering engineers to develop pipelines and structures capable of enduring such thermal fluctuations.

The graphical depiction of the transmission of the weld from the location where it was performed to the main body of the pipe is shown in Fig. 4. According to the numerical data, the temperature reaches 507 °C at the welding area, whereas it only reaches 150 °C at the heat-affected zone (HAZ). The temperature of the remaining parts of the body is within the usual range, which is 20 °C.

From a practical standpoint, it is crucial to take into account the thermal impacts that occur during the welding process and to develop structures that possess the capability to withstand the temperature gradients that are linked with it. In addition, the numerical findings that have been confirmed provide confirmation of the simulation model's correctness. These results may be utilized as a foundation for making well-informed judgments pertaining to material selection, welding processes, and overall structural integrity.

### 5. 2. Heat flux due to temperature

Fig. 5 illustrates the influence of heat flux resulting from the welding process, whereby the center point is emphasized in red to indicate the highest concentration of heat at that particular position. The thermal energy then spreads to the next region with a decreasing impact. The region in close proximity is commonly referred to as the Heat-Affected Zone (HAZ). The computational investigation of this event was helped by employing a mix of static structural and thermal transient techniques included in the Ansys program. This methodology enables a thorough investigation of the structural reaction and dynamic thermal behavior that arise from the welding procedure. The visual depiction presented in Fig. 5 provides a significant perspective on the spatial arrangement of thermal impacts, informing engineering choices pertaining to the choice of materials, considerations in design, and the overall durability of the structure.

Three-dimensional ($X$, $Y$, $Z$) numerical investigation of directional heat flux has yielded good results. The maximal heat flux is observed in the X direction, reaching 7e6 W·m$^{-2}$. This value reaches its maximum at a temperature of 500 °C. In contrast, the minimal value for the $X$ direction is 5.5e-6 W·m$^{-2}$. In the $Y$ direction, the maximum heat flux of 6.2e6 W·m$^{-2}$ occurs at 500 °C, while it decreases to a minimum of 5.6e6 W·m$^{-2}$ at 100 °C. Notably, the $Z$ direction has the narrowest range of heat flux values, with a zenith value of 6e6 W·m$^{-2}$ at 500 °C and a nadir value of 5.4e6 W·m$^{-2}$ at 100 °C. These exhaustive results illustrate the intricate spatial and thermal dynamics, highlighting the impact of both temperature and direction on the distribution of heat. These insights contribute to the optimization of material performance, structural design, and thermal management strategies in welding applications as shown in Fig. 6.

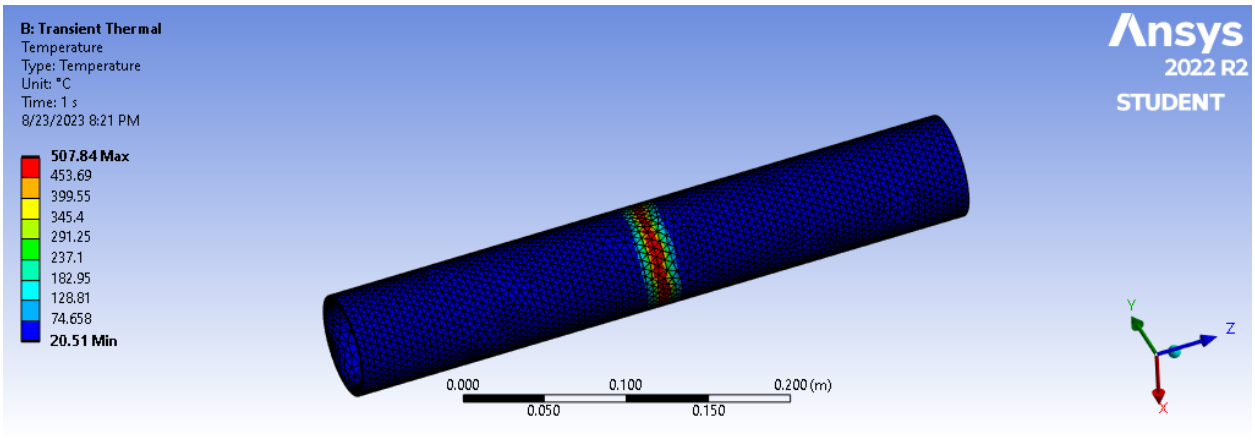


Fig. 4. Numerical representation of the distribution of temperature

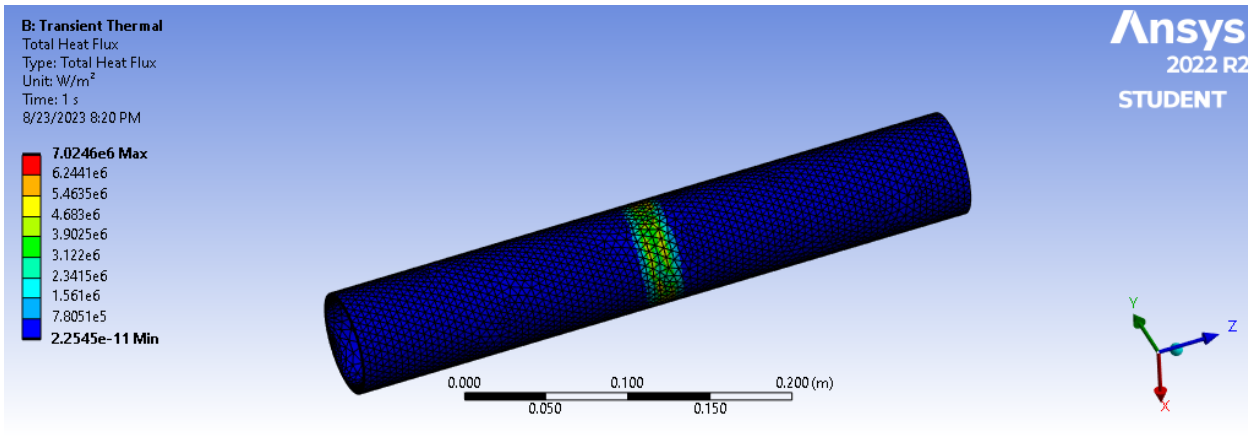


Fig. 5. Illustration of numerical results of total heat flux

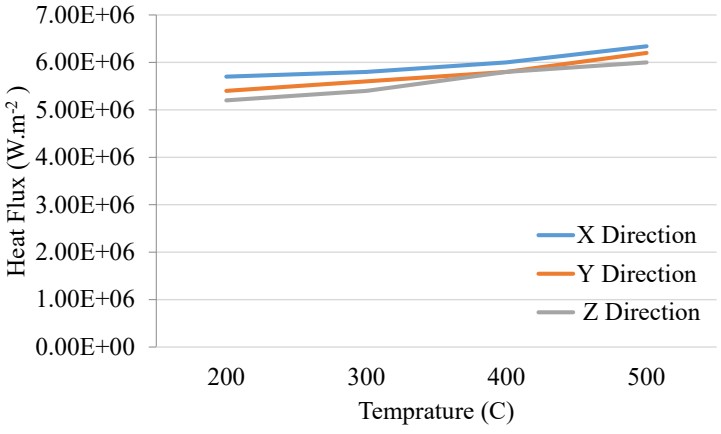


Fig. 6. Numerical results of directional heat flux

When evaluating the thermal qualities of the welding quality through the use of heat flux, three criteria were taken into consideration.

**5. 3. Residual stresses in the welded spot**

The numerical results have shown that there are redial stress dues the heating process. Fig. 7 shows the graphical effect of welding temperature to the stress of the body. The max stress is 2.5 e6 Pa. It clear that the max residual stress occurred at the edge of pipe.

The examination of stress distribution, employing the Von Mises stress criteria, in conjunction with the applied temperature, leads to valuable insights. At the location of welding, where the temperature reaches its maximum of 507 °C, the Von Mises stress attains a maximum value of 2.5e6 Pa. The significant degree of stress experienced can be attributed to the thermal effects that are generated during the welding process. A negative relationship is seen between temperature and stress, suggesting a link between these two variables. As an illustration, as the temperature reaches 100 °C, the tension decreases to 2.2e6 Pa as shown in Fig. 8.

The observed correlation between stress and temperature can be ascribed to the material's reaction to variations in thermal conditions.

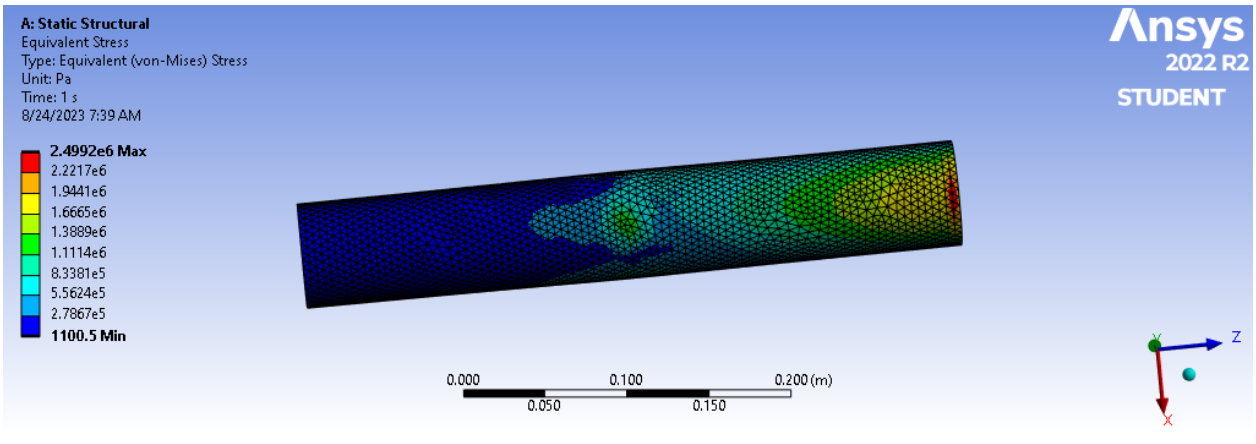


Fig. 7. Numerical illustration of Von Mises stress

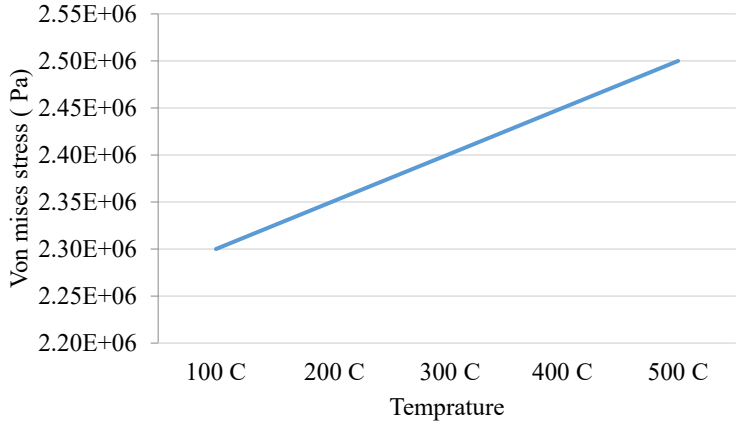


Fig. 8. Numerical results of von Mises stresses

During the welding process, the pipe experiences localized heating, which results in thermal expansion and non-uniform deformation. As a consequence, there is a formation of stress concentrations in regions that are subjected to elevated temperatures. The Von Mises stress is a metric that quantifies the combined effects of tensile and shear stresses, hence identifying areas of possible failure or regions of interest in the material.

The observed reduction in stress levels with decreasing temperature can be attributed to the dissipation of thermal effects. Lower temperatures can cause a decrease in thermal expansion and contraction, resulting in a reduction of stress concentrations. The significance of evaluating the structural integrity of welded components is emphasized by the stress-temperature relationship, highlighting the need to take into account both thermal and mechanical aspects.

## 6. Discussion of the influence of heat transfer in the welded joint of SUS304 pipe

Three parameters for the thermal performer importer were determined. The weld residual stress, heat flux due to temperature changes, and overall heat transfer efficiency are all studied.

After welding, the SUS304 pipe in Fig. 3 exhibits accurate temperature measurements all along its length. It is heated to 507 °C at the welding joint 200 mm from one end of the 400 mm pipe. From the point of welding to the border of the pipe, the temperature gradually drops. The weld spot is 500 °C, whereas the pipe's outside diameter is just 20 °C.

In Fig. 5, the red central area represents the area where the welding heat flux is most concentrated. Less force is required to transfer heat. The Heat Affected Region is close by. Directional heat flow has been quantitatively explored in *X*, *Y*, and *Z* dimensions with promising outcomes. The maximum heat flow in the *X* direction is 7e6 $W \cdot m^{-2}$. The maximum temperature is 500 °C. 5.50e-6 $W \cdot m^{-2}$ is the smallest *X* direction. There is a maximum Y-direction heat flow of 6.2e6 $W \cdot m^{-2}$ at 500 °C and a minimum of 5,6e6 $W \cdot m^{-2}$ at 100 °C. The temperature range with the lowest heat flow is at *Z*, where it peaks at 6e6 $W \cdot m^{-2}$ at 500 °C and drops to 5.4e6 at 100 °C. In Fig. 6, it is possible to see the complicated spatial and thermal dynamics influenced by temperature and orientation.

Von Mises stress criterion and applied temperature stress distribution analysis generate relevant data. Von Mises stress maximum at 507 °C welding 2.5e6 Pa. Stressful welding thermal reactions. Temperature inversely affects stress, suggesting a relationship. At 100 °C, tension drops to 2.2e6 Pa (Fig. 8). Stress-temperature connection owing to material temperature sensitivity. Piping expands and deforms due to localized welding temperature. High temperatures concentrate tension. Von Mises stress assesses tensile and shear stresses to signal material interest or failure.

The numerical results of the current analysis have been compared to the study of [34–38]. Where results have been from ANSYS using static structure tool along with thermal analysis of SUS304 pipe-welded joints has various advantages. Our technique uses static structural and thermal tools and boundary conditions for a complete study. This method's precision and accuracy, verified by validation studies, are considered.

The scope of this investigation was restricted to the use of ANSYS software for performing numerical simulations and analyses of heat transmission and stress distribution in the welded joints formed by SUS304 pipes. The modeling approach was simplified, assumptions were made regarding material parameters and boundary conditions, there was no experimental validation, and the focus was on certain welding settings and scenarios.

This study presents several notable disadvantages that can guide improvements in future research. Firstly, the reliance on simplifications and assumptions in numerical modeling introduces potential inaccuracies, which can be mitigated through more complex and realistic modeling approaches in subsequent studies. The absence of experimental validation diminishes confidence in the numerical findings, emphasizing the need for future research to incorporate experimental data for validation and real-world applicability. Additionally, the limited scope of this study, focusing on specific welding conditions and scenarios, suggests the importance of broadening the research scope to encompass a wider range of welding techniques, materials, and environmental factors. Lastly, considering more realistic boundary conditions, including mechanical loading, vibration, and environmental effects, can enhance the practical relevance and comprehensiveness of future investigations into welded joint behavior.

There is hope that improved understanding of heat transfer and stress Insights into heat transport and stress distribution in welded joints may become more exact and helpful as a result of the study's advancement. However, this research trip could have a variety of obstacles to overcome. It is not uncommon for scientists to have difficulty modeling complex processes, solving difficult equations, and running multi-physics simulations. Experimentation may be hindered by factors such as the absence of specialized equipment, insufficient data collection, and an inability to precisely replicate real-world welding conditions. Calibration and verification of numerical models against experimental data can be challenging due to computational requirements and the necessity for multidisciplinary collaboration. Researchers also need to examine ethics and safety, as well as analyze massive datasets. Despite these difficulties, businesses and applications that rely on reliable welding processes can benefit from a comprehensive and multidisciplinary approach to studying welded joint behavior.

## 7. Conclusion

1. The effectiveness of heat transfer during the welding process has been the subject of an investigation. The 400 mm pipe is heated to 507 °C at the welding joint that is located 200 mm from one end. As one moves from the welding to the pipe edge, the temperature gradually drops. Temperature is 195 mm away from the welding location and reads 500 °C, whereas the temperature at the pipe's perimeter reads 20 °C.

2. Three different approaches have been utilized in the investigation of heat flux due to temperature. The directional flow of heat has been quantitatively investigated in the dimensions *X*, *Y*, *Z*, and the results have been found to be satisfactory. The maximum amount of heat that may flow in the *X* direction is 7e6 $W \cdot m^{-2}$. At 500 °C, the va-

lues are at their highest point. The least amount of energy in the *X* direction is 5.5e-6 $W \cdot m^{-2}$. The *Y*-direction heat flow reaches its maximum of 6.2e6 $W \cdot m^{-2}$ at a temperature of 500 °C and gradually decreases to 5.6e6 when the temperature lowers to 100 °C. *Z* has the narrowest temperature range for its heat flux, which reaches its highest point of 6e6 $W \cdot m^{-2}$ at 500 °C and its lowest point of 5.4e6 at 100 °C.

3. The von Mises stress has been taken into consideration as a potential signal for the Residual Stresses in the area where the weld was made. The Von Mises stress at its highest at 507 °C was 2.5e6 Pa. Thermal responses under stress caused by welding. There is a correlation between stress and temperature because temperature has an opposing effect on stress. The stress is reduced to 2.2e6 Pa when the temperature reaches 100 °C.

## Conflict of interest

The authors declare that they have no conflict of interest in relation to this research, whether financial, personal, authorship or otherwise, that could affect the research and its results presented in this paper.

## Financing

The study was performed without financial support.

## Data availability

Data will be made available on reasonable request.

References

1. Savin, V. V., Lebedeva, K. N., Herelovich, V. V., Savina, L. A., Chaika, V. A. (2020). Prospects for the use of u-shaped welded pipes of steel a316l heat transfer assortment in chemical engineering. IOP Conference Series: Materials Science and Engineering, 939 (1), 012069. doi: https://doi.org/10.1088/1757-899x/939/1/012069
2. Yang, Z., Fang, Y., He, J. (2020). Numerical simulation of heat transfer and fluid flow during vacuum electron beam welding of 2219 aluminium girth joints. Vacuum, 175, 109256. doi: https://doi.org/10.1016/j.vacuum.2020.109256
3. Ji, Y., Yuan, D., Hao, Y., Tian, Z., Lou, J., Wu, Y. (2022). Experimental study on heat transfer performance of high temperature heat pipe with large length-diameter ratio for heat utilization of concentrated solar energy. Applied Thermal Engineering, 215, 118918. doi: https://doi.org/10.1016/j.applthermaleng.2022.118918
4. Peng, X., Xu, G., Zhou, A., Yang, Y., Ma, Z. (2020). An adaptive Bernstein-Bézier finite element method for heat transfer analysis in welding. Advances in Engineering Software, 148, 102855. doi: https://doi.org/10.1016/j.advengsoft.2020.102855
5. Ham, J., Shin, Y., Cho, H. (2019). Theoretical investigation of the influence of pipe diameter and exit channel width in welded plate heat exchanger on heat exchanger performance. Heat and Mass Transfer, 56 (3), 759–771. doi: https://doi.org/10.1007/s00231-019-02733-8
6. Sharaf, H. K., Salman, S., Abdulateef, M. H., Magizov, R. R., Troitskii, V. I., Mahmoud, Z. H. et al. (2021). Role of initial stored energy on hydrogen microalloying of ZrCoAl(Nb) bulk metallic glasses. Applied Physics A, 127 (1). doi: https://doi.org/10.1007/s00339-020-04191-0
7. Yao, Y., Ding, J., Zhang, Y., Wang, W., Lu, J. (2023). Thermal and hydraulic optimization of supercritical CO2 pillow plate heat exchanger with ellipse weld spots in CSP system. International Communications in Heat and Mass Transfer, 143, 106739. doi: https://doi.org/10.1016/j.icheatmasstransfer.2023.106739
8. Der, O., Alqahtani, A. A., Marengo, M., Bertola, V. (2021). Characterization of polypropylene pulsating heat stripes: Effects of orientation, heat transfer fluid, and loop geometry. Applied Thermal Engineering, 184, 116304. doi: https://doi.org/10.1016/j.applthermaleng.2020.116304
9. Markushin, M. E., Galanskiy, S. A., Maksimov, I. S., Zolkin, A. L. (2023). Passive control of a temperature of continuous welded rail using loop heat pipes. AIP Conference Proceedings. doi: https://doi.org/10.1063/5.0162725
10. Sharaf, H. K., Salman, S., Dindarloo, M. H., Kondrashchenko, V. I., Davidyants, A. A., Kuznetsov, S. V. (2021). The effects of the viscosity and density on the natural frequency of the cylindrical nanoshells conveying viscous fluid. The European Physical Journal Plus, 136 (1). doi: https://doi.org/10.1140/epjp/s13360-020-01026-y
11. Liu, Y., Wang, P., Fang, H., Ma, N. (2021). Mitigation of residual stress and deformation induced by TIG welding in thin-walled pipes through external constraint. Journal of Materials Research and Technology, 15, 4636–4651. doi: https://doi.org/10.1016/j.jmrt.2021.10.035
12. Zhao, J., Ji, Y., Yuan, D.-Z., Guo, Y.-X., Zhou, S.-W. (2022). Structural effect of internal composite wick on the anti-gravity heat transfer performance of a concentric annular high-temperature heat pipe. International Communications in Heat and Mass Transfer, 139, 106404. doi: https://doi.org/10.1016/j.icheatmasstransfer.2022.106404
13. Sharaf, H. K., Ishak, M. R., Sapuan, S. M., Yidris, N. (2020). Conceptual design of the cross-arm for the application in the transmission towers by using TRIZ–morphological chart–ANP methods. Journal of Materials Research and Technology, 9 (4), 9182–9188. doi: https://doi.org/10.1016/j.jmrt.2020.05.129
14. Abdullah, Y. M., Aziz, G. S., Sharaf, H. K. (2023). Simulate the Rheological Behaviour of the Solar Collector by Using Computational Fluid Dynamic Approach. CFD Letters, 15 (9), 175–182. doi: https://doi.org/10.37934/cfdl.15.9.175182

15. Yu, J., Xin, Z., Zhang, R., Chen, Z., Li, Y., Zhou, W. (2022). Effect of spiral woven mesh liquid pumping action on the heat transfer performance of ultrathin vapour chamber. International Journal of Thermal Sciences, 182, 107799. doi: https://doi.org/10.1016/j.ijthermalsci.2022.107799
16. Sharaf, H. K., Alyousif, S., Khalaf, N. J., Hussein, A. F., Abbas, M. K. (2022). Development of bracket for cross arm structure in transmission tower: Experimental and numerical analysis. New Materials, Compounds and Applications, 6 (3), 257–275. Available at: http://jomardpublishing.com/UploadFiles/Files/journals/NMCA/V6N3/SharafHS.pdf
17. Liu, Y., Yu, Y., Wang, P., Fang, H., Ma, N. (2022). Analysis and mitigation of the bending deformation in girth-welded slender pipes with numerical modelling and experimental measurement. Journal of Manufacturing Processes, 78, 278–287. doi: https://doi.org/10.1016/j.jmapro.2022.04.023
18. Sharaf, H. K., Ishak, M. R., Sapuan, S. M., Yidris, N., Fattahi, A. (2020). Experimental and numerical investigation of the mechanical behavior of full-scale wooden cross arm in the transmission towers in terms of load-deflection test. Journal of Materials Research and Technology, 9 (4), 7937–7946. doi: https://doi.org/10.1016/j.jmrt.2020.04.069
19. Liu, Y., Wang, P., Fang, H., Ma, N. (2021). Characteristics of welding distortion and residual stresses in thin-walled pipes by solid-shell hybrid modelling and experimental verification. Journal of Manufacturing Processes, 69, 532–544. doi: https://doi.org/10.1016/j.jmapro.2021.08.014
20. Almagsoosi, L., Abadi, M. T. E., Hasan, H. F., Sharaf, H. K. (2022). Effect of the Volatility of the Crypto Currency and Its Effect on the Market Returns. Industrial Engineering & Management Systems, 21 (2), 238–243. doi: https://doi.org/10.7232/iems.2022.21.2.238
21. Al-Fahad, I. O. B., Sharaf, H. kadhim, Bachache, L. N., Bachache, N. K. (2023). Identifying the mechanism of the fatigue behavior of the composite shaft subjected to variable load. Eastern-European Journal of Enterprise Technologies, 3 (7 (123)), 37–44. doi: https://doi.org/10.15587/1729-4061.2023.283078
22. Chen, G., Tang, Y., Wan, Z., Zhong, G., Tang, H., Zeng, J. (2019). Heat transfer characteristic of an ultra-thin flat plate heat pipe with surface-functional wicks for cooling electronics. International Communications in Heat and Mass Transfer, 100, 12–19. doi: https://doi.org/10.1016/j.icheatmasstransfer.2018.10.011
23. Gharib, A. R., Biglari, F. R., Shafaie, M., Kokabi, A. H. (2019). Experimental and numerical investigation of fixture time on distortion of welded part. The International Journal of Advanced Manufacturing Technology, 104 (1-4), 1121–1131. doi: https://doi.org/10.1007/s00170-019-03874-0
24. Kong, Y. S., Cheepu, M., Park, Y. W. (2020). Effect of Heating Time on Thermomechanical Behavior of Friction-Welded A105 Bar to A312 Pipe Joints. Transactions of the Indian Institute of Metals, 73 (6), 1433–1438. doi: https://doi.org/10.1007/s12666-020-01900-4
25. Mikulionok, I. O. (2019). Classification of Means of Enhancement of Heat Transfer from the Outer Surface of Pipes (Survey of Patents). Chemical and Petroleum Engineering, 55 (5-6), 491–499. doi: https://doi.org/10.1007/s10556-019-00651-4
26. Liu, R.-F., Wang, J.-C. (2022). Application of finite element method to effect of weld overlay residual stress on probability of piping failure. International Journal of Pressure Vessels and Piping, 200, 104812. doi: https://doi.org/10.1016/j.ijpvp.2022.104812
27. Raheemah, S. H., Fadheel, K. I., Hassan, Q. H., Aned, A. M., Turki Al-Taie, A. A., Sharaf, H. K. (2021). Numerical Analysis of the Crack Inspections Using Hybrid Approach for the Application the Circular Cantilever Rods. Pertanika Journal of Science and Technology, 29 (2). doi: https://doi.org/10.47836/pjst.29.2.22
28. Raheemah, S. H., Ashham, M. A., Salman, K. (2019). Numerical investigation on enhancement of heat transfer using rod inserts in single pipe heat exchanger. Journal of Mechanical Engineering and Sciences, 13 (4), 6112–6124. doi: https://doi.org/10.15282/jmes.13.4.2019.24.0480
29. Asadi, P., Alimohammadi, S., Kohantorabi, O., Soleymani, A., Fazli, A. (2020). Numerical investigation on the effect of welding speed and heat input on the residual stress of multi-pass TIG welded stainless steel pipe. Proceedings of the Institution of Mechanical Engineers, Part B: Journal of Engineering Manufacture, 235 (6-7), 1007–1021. doi: https://doi.org/10.1177/0954405420981335
30. Salman, S., Sharaf, H. K., Hussein, A. F., Khalaf, N. J., Abbas, M. K., Aned, A. M. et al. (2022). Optimization of raw material properties of natural starch by food glue based on dry heat method. Food Science and Technology, 42. doi: https://doi.org/10.1590/fst.78121
31. Salman, K. h., Elsheikh, A. H., Ashham, M., Ali, M. K. A., Rashad, M., Haiou, Z. (2019). Effect of cutting parameters on surface residual stresses in dry turning of AISI 1035 alloy. Journal of the Brazilian Society of Mechanical Sciences and Engineering, 41 (8). doi: https://doi.org/10.1007/s40430-019-1846-0
32. Arora, H., Mahaboob Basha, K., Naga Abhishek, D., Devesh, B. (2022). Welding simulation of circumferential weld joint using TIG welding process. Materials Today: Proceedings, 50, 923–929. doi: https://doi.org/10.1016/j.matpr.2021.06.315
33. Lavrentieva, O. O., Arkhypov, I. O., Kuchma, O. I., Uchitel, A. D. (2020). Use of simulators together with virtual and augmented reality in the system of welders' vocational training: past, present, and future. doi: https://doi.org/10.31812/123456789/3748
34. Alyaseri, N. H. A., Salman, M. D., Maseer, R. W., Hussein, E. K., Subhi, K. A., Alwan, S. A. et al. (2023). Exploring the Modeling of Socio-Technical Systems in the Fields of Sport, Engineering and Economics. Revista iberoamericana de psicología del ejercicio y el deporte, 18 (3), 338–341. Available at: https://dialnet.unirioja.es/servlet/articulo?codigo=9087565

35. Jawad, K. K., Alyaseri, N. H. A., Alwan, S. A., Hussein, E. K., Subhi, K. A., Sharaf, H. K. et al. (2023). Contingency in Engineering Problem Solving Understanding its Role and Implications: Focusing on the sports Machine. Revista iberoamericana de psicología del ejercicio y el deporte, 18 (3), 334–337. Available at: https://dialnet.unirioja.es/servlet/articulo?codigo=9087564
36. Salman, M. D., Alwan, S. A., Alyaseri, N. H. A., Subhi, K. A., Hussein, E. K., Sharaf, H. K. et al. (2023). The Impact of Engineering Anxiety on Students: A Comprehensive Study In the fields of Sport, economics, and teaching methods. Revista iberoamericana de psicología del ejercicio y el deporte, 18 (3), 326–329. Available at: https://dialnet.unirioja.es/servlet/articulo?codigo=9087521
37. Alwan, S. A., Jawad, K. K., Alyaseri, N. H. A., Subhi, K. A., Hussein, E. K., Aned, A. M. et al. (2023). The Psychological Effects of Perfectionism on Sport, economic and Engineering Students. Revista iberoamericana de psicología del ejercicio y el deporte, 18 (3), 330–333. Available at: https://dialnet.unirioja.es/servlet/articulo?codigo=9087522
38. Al-Fahad, I. O. B., Hassan, A. D., Faisal, B. M., Sharaf, H. kadhim. (2023). Identification of regularities in the behavior of a glass fiber-reinforced polyester composite of the impact test based on ASTM D256 standard. Eastern-European Journal of Enterprise Technologies, 4 (7 (124)), 63–71. doi: https://doi.org/10.15587/1729-4061.2023.286541